Inorganic Chemistry
Article
Cite This: Inorg. Chem. XXXX, XXX, XXX−XXX
pubs.acs.org/IC

Electronic Energy Transduction from {Ru(py)$_4$} Chromophores to Cr(III) Luminophores

Alejandro Cadranel,*[,†,‡] Paola S. Oviedo,[†] Pablo Alborés,[†] Luis M. Baraldo,[†] Dirk M. Guldi,[‡] and José H. Hodak*[,†]

[†]Departamento de Química Analítica, Inorgánica y Química Física & INQUIMAE, Facultad de Ciencias Exactas y Naturales, Universidad de Buenos Aires, Pabellón 2, Ciudad Universitaria, C1428EHA Buenos Aires, Argentina

[‡]Department of Chemistry and Pharmacy & Interdisciplinary Center for Molecular Materials (ICMM), Friedrich-Alexander-Universität Erlangen-Nürnberg, Egerlandstraße 1-3, 91058 Erlangen, Germany

Supporting Information

ABSTRACT: Despite the large body of work on {Ru(bpy)$_2$} sensitizer fragments, the same attention has not been devoted to their {Ru(py)$_4$} analogues. In this context, we explored the donor−acceptor *trans*-[Ru(L)$_4${(μ-NC)Cr(CN)$_5$}$_2$]$^{4-}$, where L = pyridine, 4-methoxypyridine, 4-dimethylaminopyridine. We report on the synthesis and the crystal structure as well as the electrochemical, spectroscopical, and photophysical properties of these trimetallic complexes, including transient absorption measurements. We observed emission from chromium-centered d−d states upon illuminating into either MLCT or MM′CT absorptions of {Ru(L)$_4$} or {Ru-Cr}, respectively. The underlying energy transfer is as fast as 600 fs with quantum efficiencies ranging from 10% to 100%. These results document that {Ru(py)$_4$} sensitizer fragments are as efficient as {Ru(bpy)$_2$} in short-range energy transfer scenarios.

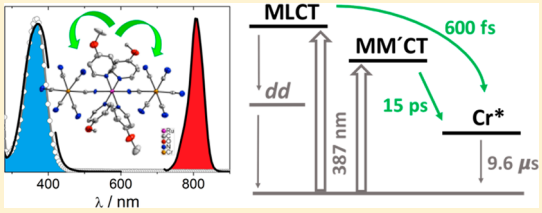

INTRODUCTION

[Ru(bpy)$_3$]$^{2+}$ has been the benchmark for inorganic photochemistry in recent decades. Facile synthesis procedures and wide tunability of their excited-state energies resulted in the omnipresence of [Ru(bpy)$_3$]$^{2+}$ and its derivatives. Numerous derivatives of [Ru(bpy)$_3$]$^{2+}$ were designed either to answer fundamental questions or to advance technological devices.[1−5] Of great relevance is the {Ru(bpy)$_2$} fragment,[6,7] owing to the fact that it retains many of the remarkable characteristics of [Ru(bpy)$_3$]$^{2+}$ and offers, at the same time, two coordination sites to add specific properties or functions. Despite the extensive and diverse studies performed on {Ru(bpy)$_2$}, {Ru(py)$_4$} has been less frequently explored. Possibly the short-lived MLCT excited states,[8] the nonemissivity at room temperature,[8] and the blue-shifted absorptions[9] hampered scientific interest in these fragments.

However, {Ru(py)$_4$} bears a myriad of intriguing properties. For example, pyridinic ligands with a variety of substituents at the 4-position are employable toward tuning the electronic structure.[10−14] Equally versatile are their solvento complexes as precursors as a means to realize unsymmetrically trans disubstituted {Ru(py)$_4$}.[15−17] A stable trans configuration[9] assists in overcoming the steric constraints typically encountered in *cis*-{Ru(bpy)$_2$}, especially when larger bridged systems or densely covered surfaces are at stake.[18] Diverse molecular architectures were built around these building blocks,[11,19−22] and cyanide-bridged molecular wires stand as notable examples.[23,24] Such a cyanide-based motif enables strong electronic coupling between the metal centers without detrimental traps or low-energy states that impede any efficient energy or charge migration.[25−27]

Chromium(III) complexes are also a playground for photochemists.[28−34] The most studied Cr(III)-based systems include polypyridines[35−41] and fragments such as {Cr(CN)$_6$}[42−46] and {Cr(aza-macrocycle)}.[47−54] They have been exploited as sensitizers or luminophores, not only in solution but also in the solid state.[55] They have been designed in search for hole transfer to semiconductor substrates[56] and for their use in upconversion schemes.[57,58] Chromium(III) complexes also play an important role as earth-abundant materials in photocatalysis,[59−63] due to the combination of high oxidation power and long lifetime of their excited states.[36,56,64−69] In general, emissive metal-centered (ligand field) excited states, labeled Cr*, dominate the photophysics of Cr(III) fragments. In an octahedral field, the ground-state electronic configuration of Cr(III) is t_{2g}^3, while the emissive ^2E_g state corresponds to an intraconfigurational spin flip from the ground $^4A_{2g}$ state. Emission occurs without major nuclear rearrangements due to the fact that the associated potential energy surfaces are nested. In solution, Cr* emissions are spectrally narrow and long-lived, especially in comparison with typical MLCT emissions.[28,33,70] Transient absorption spectroscopy of these excited states has been studied on different time scales for monometallic complexes,[70,71] but reports on supramolecular systems are still scarce.[44−46]

Received: November 2, 2017

DOI: 10.1021/acs.inorgchem.7b02799
Inorg. Chem. XXXX, XXX, XXX−XXX

In this context, {Ru-Cr} systems are an interesting platform for studying fundamental photoinduced processes, especially for developing chromophore−catalyst assemblies. Of great relevance is transient absorption spectroscopy, which enables detailed insights into the dynamics and the nature of the excited states. Following this notion, we report in this work *for the first time* on the {Ru(py)$_4$} photosensitization in novel *trans*-[Ru(L)$_4${(μ-NC)Cr(CN)$_5$}$_2$]$^{4-}$ trimetallic complexes (L = pyridine, 4-methoxypyridine, 4-dimethylaminopyridine; see Figure 1). Notably, their acceptor−donor−acceptor configuration sets up the ways and means for an effective energy transfer to {Cr(CN)$_6$} luminophores. For {Ru(bpy)$_2$}, no major differences were observed between trimetallic {Cr-Ru-Cr} and bimetallic {Ru-Cr} complexes.[44] Thus, we opted in the current work to investigate trimetallic {Cr-Ru-Cr}.

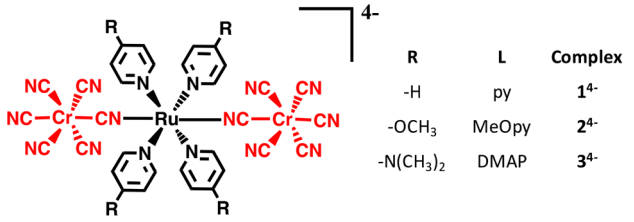

Figure 1. Molecular structures of the *trans*-[Ru(L)$_4${(μ-NC)Cr(CN)$_5$}$_2$]$^{4-}$ complexes reported in this work. Acceptor fragments are shown in red, while the donor fragment is given in black.

EXPERIMENTAL SECTION

Materials. *trans*-[Ru(py)$_4$Cl$_2$],[9] *trans*-[Ru(MeOpy)$_4$Cl$_2$],[12] [Ru(DMAP)$_6$]Cl$_2$,[72] and K$_3$[Cr(CN)$_6$][73] were prepared according to literature procedures. Solvents for electrochemical and spectral measurements were dried using a PureSolv Micro solvent purification system. All other reagents were obtained commercially and used as supplied. The compounds synthesized were dried in a vacuum desiccator for at least 12 h prior to their characterization.

Synthesis of the Complexes. *(PPh$_4$)$_3$[Cr(CN)$_6$].* In a typical preparation, 30 mmol (9.8 g) of K$_3$[Cr(CN)$_6$] were dissolved in 50 mL of water and 93 mmol (35 g) of solid tetraphenylphosphonium chloride were added. The resulting suspension was vigorously stirred in the dark for about 2 h. The obtained solid was filtered, washed with water, and vacuum-dried. Yield: 25.8 g (70%). Anal. Calcd for [Cr(CN)$_6$](Ph$_4$P)$_3$·0.2H$_2$O, C$_{78}$H$_{64}$N$_6$O$_2$P$_3$Cr: C, 74.2; H, 4.8; N, 6.7. Found: C, 73.8; H, 5.0; N, 6.5. ν(CN): 2111 (s) cm^{-1}, 2130 (s) cm^{-1}.

*trans-[L$_4$Ru^{II}{(μ-NC)Cr^{III}(CN)$_5$}$_2$](PPh$_4$)$_4$ (L = Pyridine (**1(PPh$_4$)$_4$**), 4-Methoxypyridine (**2(PPh$_4$)$_4$**)).* In a typical preparation, 2 mmol of *trans*-[Ru(L)$_4$Cl$_2$] and a large excess of K$_3$[Cr(CN)$_6$] (6.5 g, 20 mmol) were suspended in 250 mL of a water/methanol mixture (1/2 v/v). The resulting suspension was heated to reflux for 4 h in the dark with vigorous stirring. Along the course of the reaction, the ruthenium precursor completely dissolved, yielding a deep orange solution. When it was cooled to room temperature, the solution was evaporated to dryness under reduced pressure. The orange solid residue was extracted with methanol, and most of the unreacted K$_3$[Cr(CN)$_6$] was removed by filtration. The deep red extracted methanolic solution was evaporated to dryness under reduced pressure, and the solid residue was dissolved in a minimum amount of water to afford a purple reddish solution. After addition of 4 g of solid tetraphenylphosphonium chloride, a bulky yellow solid precipitated, which was filtered off, thoroughly washed with water, and vacuum-dried.

This crude solid was purified by exclusion chromatography using a Sephadex LH-20 column (l = 60 cm, ϕ = 4 cm) packed and eluted with methanol. The third colored fraction, which eluted from the column, was collected and evaporated to dryness, and the light orange solid was dried under vacuum. Further purification was achieved by recrystallization from methanol/ether. Yields: 40% (L = py) and 54% (L= 4-MeOpy). Anal. Calcd for **1(PPh$_4$)$_4$·8H$_2$O**, C$_{128}$H$_{116}$N$_{16}$O$_8$P$_4$Cr$_2$Ru: C, 65.8; H, 5.0; N, 9.6. Found: C, 65.9; H, 5.0; N, 10.1. ν(CN): 2121 (s) cm^{-1}. Anal. Calcd for **2(PPh$_4$)$_4$·4H$_2$O**, C$_{132}$H$_{116}$N$_{16}$O$_8$P$_4$Cr$_2$Ru: C, 66.5; H, 4.9; N, 9.4. Found: C, 66.6; H, 5.1; N, 9.3. ν(CN): 2116 (s) cm^{-1}.

*trans-[(DMAP)$_4$Ru^{II}{(μNC)Cr^{III}(CN)$_5$}$_2$](PPh$_4$)$_4$ (**3(PPh$_4$)$_4$**).* A 210 mg portion (0.2 mmol) of [Ru(DMAP)$_6$]Cl$_2$·9H$_2$O was dissolved in 10 mL of absolute ethanol. To this solution was added 2 g (1.6 mmol) of (PPh$_4$)$_3$[Cr(CN)$_6$] dissolved in 5 mL of absolute ethanol. A voluminous solid was immediately formed. This suspension was heated to reflux in the dark with vigorous stirring. After 10 min, the suspended solid was completely dissolved, and after 1/2 h a new solid appeared. This latter suspension was further heated for 15 min and then cooled to room temperature. The product was filtered, washed with cold absolute ethanol (3 × 10 mL), and vacuum-dried. Yield: 360 mg (76%). Anal. Calcd for **3(PPh$_4$)$_4$·5H$_2$O**, C$_{136}$H$_{130}$N$_{20}$O$_5$P$_4$Cr$_2$Ru: C, 66.6; H, 5.0; N, 11.4. Found: C, 66.7; H, 4.9; N, 11.7. ν(CN): 2114 (s) cm^{-1}.

Physical Measurements. IR spectra were collected on a Shimadzu Prestige 21 instrument in ATR mode or in the form of KBr pellets using a Nicolet FTIR 510P spectrometer. UV−visible spectra were recorded with a Hewlett-Packard 8453 diode array spectrometer (range 190−1100 nm). Elemental analyses were carried on a Carlo Erba 1108 analyzer with an estimated error of ±0.5%. Electrochemical measurements were performed under argon with millimolar solutions, using a TEQ V3 potentiostat and a standard three-electrode arrangement consisting of a glassy-carbon disk (area 9.4 mm^2) as the working electrode, a platinum wire as the counter electrode, and a silver wire as the reference electrode plus an internal ferrocene (Fc) standard. Tetra-*n*-butylammonium hexafluorophosphate ([TBA]PF$_6$, 0.1 M) was used as the supporting electrolyte. All potentials are referenced to the standard Ag/AgCl saturated KCl electrode (0.197 V vs NHE), the conversions being performed with literature values for the Fc$^+$/Fc couple.[74] Excitation and emission spectra were recorded with a PTI-QuantaMaster or a Cary Eclipse spectrofluorimeter. Quantum yields were measured in argon-saturated solutions using [Ru(bpy)$_3$]$^{2+}$ (φ = 0.095[75] in ACN at 25 °C) and [Cr(CN)$_6$]$^{3-}$ (φ = 1.7 × 10^{-3} in DMF[44] at 25 °C) as references. For luminescence lifetime measurements, excitation was done with the output of a femtosecond optical parametric amplifier at 350 nm (<200 fs fwhm pulses). The emission light was collected with a 5 cm focal length lens focused on the entrance of a monochromator (Oriel 77250). The signal was detected with a photomultiplier tube (Hammamatsu R928) and a 500 MHz digitizing oscilloscope (Agilent MSO5062A).

Samples for transient absorption (TA) measurements were dissolved in thoroughly argon degassed anhydrous methanol. A flow cell having a 2 mm path length was employed (10 mL/min) to avoid possible photoproduct accumulation stemming from the population of Ru d−d states, Cr d−d states, or even dissociative CT states that bear a labile Cr(II) ion.[76−82] Ultrafast experiments were performed with an amplified Ti/sapphire laser system (Clark MXR CPA2101, fwhm = 150 fs, λ_{exc} 450 and 387 nm, 500 nJ per pulse) using transient absorption pump/probe detection systems (Helios and Eos, Ultrafast Systems). White light was generated focusing a fraction split from the fundamental beam onto sapphire. Global and target analyses were performed using the GloTarAn software and the R package TIMP.[83−85]

To quantify the energy transfer efficiencies (η_{ET}) we refer to the definition of the quantum yield

$$\varphi = \eta k_{rad} \tau$$

Comparing the emission quantum yields and lifetimes for **1**$^{4-}$−**3**$^{4-}$ and the hexacyanidochromate complex and assuming that they all have the same radiative constant (k_{rad}), we obtain

$$\eta_{ET} = \frac{\eta_{Cr}\varphi_{CrRuCr}\tau_{Cr}k_{rad}^{Cr}}{\varphi_{Cr}\tau_{CrRuCr}k_{rad}^{CrRuCr}} \approx \frac{\eta_{Cr}\varphi_{CrRuCr}\tau_{Cr}}{\varphi_{Cr}\tau_{CrRuCr}} \quad (1)$$

DOI: 10.1021/acs.inorgchem.7b02799
Inorg. Chem. XXXX, XXX, XXX−XXX

where φ_{Cr}, τ_{Cr}, and η_{Cr} are the emission quantum yield, the emission lifetime, and the quantum efficiency of populating the Cr* state in hexacyanidochromate, respectively, while φ_{CrRuCr} and τ_{CrRuCr} are the quantum yield of {Cr-Ru-Cr} emission and its lifetime. Notably, the presence of the heavy-metal ion Ru(II) is likely to enhance the k_{rad} value of the Cr* by means of spin−orbit coupling.[46] As such, η_{ET} in {Cr-Ru-Cr} trimetallic species is slightly overestimated by using eq 1.[46] Effective electronic communication between metal centers has been established in a series of $[Ru(L)_4\{(\mu\text{-NC})M\}_2]$ cyanide-bridged complexes, in which M is Fe, Ru, and Os.[11,12,20,24,86,87] Such interactions are likely to alter the electronic structure of the Cr-centered MC acceptor states and the magnitude of k_{rad}. Our estimates regarding the energy transfer efficiencies are useful for comparative analyses among trimetallic {Cr-Ru-Cr} species but should be taken carefully in a larger context.

X-ray Structure Determination. Crystals suitable for X-ray diffraction were mounted on glass fibers. The crystal structures of $\mathbf{2(PPh_4)_4}$ and $\mathbf{3(PPh_4)_4}$ were determined with a Bruker Smart APEX II CCD area-detector diffractometer using graphite-monochromated Mo Kα radiation (λ = 0.71073 Å) at 173 K. Data were corrected for absorption with PLATON[88] using a multiscan semiempirical method. The structure was solved by direct methods with SHELXS[89] and refined by full-matrix least squares on F^2 with SHELXL-2014.[89] Hydrogen atoms were added geometrically and refined as riding atoms with a uniform value of U_{iso}, with the exception of hydrogen atoms of the solvent water molecules, which could not be located in the difference map.

In the structure of $\mathbf{2}^{4-}$, the methoxy group in both pyridine ligands of the asymmetric unit were found to lay disordered around two positions and further refined with a fixed 0.5:0.5 occupancy ratio, one of them crystallographically imposed through a 2-fold rotation axis.

In the structures of both complexes most of the water and methanol solvent molecules appear heavily disordered and were refined through an ad hoc combination of split positions and fractional occupation numbers. This methodology allowed us to address most of the electron density due to the overall solvent contribution. CCDC 1408010 and 1408011 contain supplementary crystallographic data for this paper.

RESULTS

Synthesis. Following a procedure similar to that developed by some of us for the preparation of Fe-containing trinuclear complexes,[12] we extended this family to include the corresponding Cr analogues. The inertness of the hexacyanidochromate allowed us to react a large excess of it with *trans*-$[Ru(L)_4Cl_2]$ or $[Ru(DMAP)_6]^{2+}$ without forming higher oligomers. Size exclusion chromatographic purification procedures yielded $\mathbf{1}^{4-}$ and $\mathbf{2}^{4-}$, while $\mathbf{3}^{4-}$ precipitated directly from the reaction medium. The presence of unpaired electrons on the chromium centers (d^3 configuration) precluded conventional NMR characterization. However, elemental analyses and crystal structure analyses confirmed the nature of the complexes. ATR-IR spectra of the complexes are shown in Figure S1.

Crystal Structures. Slow diffusion of diethyl ether into methanolic solutions of $\mathbf{2}^{4-}$ and $\mathbf{3}^{4-}$ rendered single crystals at low temperatures, which were suitable for X-ray diffraction measurements. Figure 2 shows the crystal structures of $\mathbf{2}^{4-}$ and $\mathbf{3}^{4-}$, with the most relevant bond distances as well as angles summarized in Table 1. Crystallographic data are collected in Table S1.

In $\mathbf{2}^{4-}$ and $\mathbf{3}^{4-}$, the ruthenium ion is best described as an axially compressed coordination sphere of N atoms. Pyridines are disposed in the typical propeller-like configuration of ruthenium tetrapyridinic fragments, and $Ru-N_{py}$ bond lengths range from 2.051 to 2.097 Å.[9,12,13,86] $Ru-N_{py}$ bond lengths are

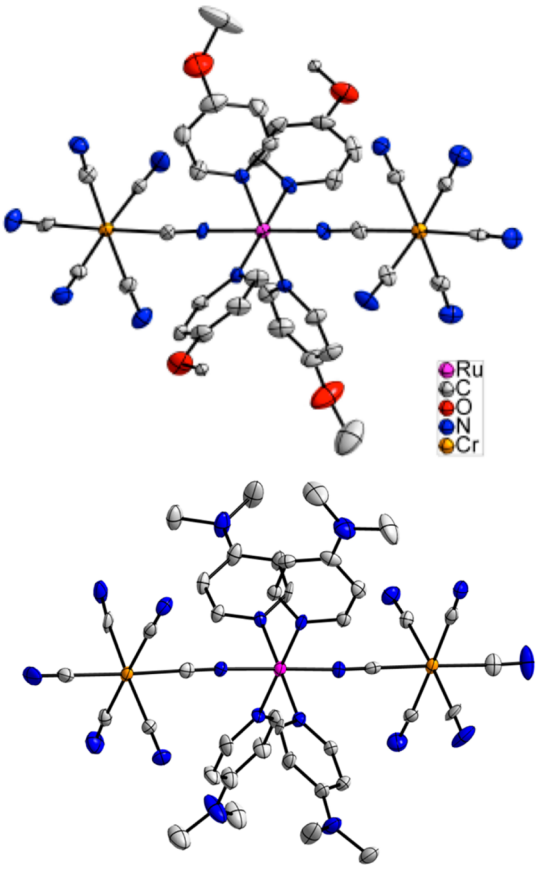

Figure 2. X-ray structures of $\mathbf{2}^{4-}$ (top) and $\mathbf{3}^{4-}$ (bottom). Ellipsoids represent 30% displacement probability. Hydrogen atoms and $P(Ph_4)^+$ counterions are omitted for clarity. Oxygen-bound methyl groups present disorder between two positions in $\mathbf{2}^{4-}$ (see text).

Table 1. Selected Bond Distances and Angles for $\mathbf{2}^{4-}$ and $\mathbf{3}^{4-}$

$\mathbf{2}^{4-}$		$\mathbf{3}^{4-}$
	Distances/Å	
	$Ru-N_{bridge}$	
2.005(7)		2.001(8)
2.005(7)		2.001(8)
	$N-C_{bridge}$	
1.146(11)		1.171(10)
1.146(11)		1.171(10)
	$Ru-N_{py}$	
2.085(10)		2.097(11)
2.076(7)		2.095(7)
2.076(7)		2.095(7)
2.051(11)		2.088(12)
	Ru−Cr	
5.201		5.234
	Angles/deg	
	$Ru-N-C_{bridge}$	
176.9(7)		176.5(6)
176.9(7)		176.5(6)
	$N-C_{bridge}-Cr$	
174.1(8)		179.0(10)
174.1(8)		179.0(10)
	$N_{bridge}-Ru-N_{bridge}$	
179.2(5)		178.9(5)
	Cr−Ru−Cr	
179.77		178.94

DOI: 10.1021/acs.inorgchem.7b02799
Inorg. Chem. XXXX, XXX, XXX−XXX

shorter for L = MeOpy, in contrast to the predictions based on the pK_b values, which are 7.4 for MeOpy and 4.3 for DMAP. Notably, DMAP is a better σ donor but also a poorer π acceptor than MeOpy, because of its higher electron density. As such, Ru−heterocycle π-back-bonding interactions are less intense in $\mathbf{3}^{4-}$ than they are in $\mathbf{2}^{4-}$. This results in $\mathbf{2}^{4-}$ in shorter and stronger Ru−N_{py} bonds, in comparison to $\mathbf{3}^{4-}$. The Ru−Cr distance is slightly greater than 5.2 Å, placing the terminal Cr ions roughly 1.04 nm apart from each other. Overall, the structures are almost linear with respect to the Cr−Ru−Cr axis, which confirms the thermal stability of the trans configuration of the {Ru(L)$_4$} fragment.

Electrochemistry. Cyclic voltammograms in acetonitrile of $\mathbf{1}^{4-}$−$\mathbf{3}^{4-}$ are shown in Figure S2 and the data are collected in Table 2. Anodic scans exhibit quasi-reversible one-electron oxidations resembling those seen for other {Ru(py)$_4$} fragments[9,12] and, in turn, are assigned to Ru-centered processes. Their values decrease as a function of the σ-donor strength/π-acceptor weakness of pyridine. Cathodic scans are consistent with Cr-centered, irreversible reductions[91] at about −1.8 V for $\mathbf{1}^{4-}$−$\mathbf{3}^{4-}$ in acetonitrile. An increase in Gutmann's acceptor number[92] of the solvent (from CH_3CN to H_2O) results in anodic shifts for the reduction of the Cr-centers. This is due to a partial donation of electron density from CN^- to the solvent, as frequently observed for {M(CN)$_6$} complexes.[12] Considering that such interactions in just the {Ru(L)$_4$} fragment are negligible, the subtle cathodic shifts for the oxidation of the Ru-centers in $\mathbf{1}$-$\mathbf{3}^{4-}$ are assigned to the electronic communication between the metallic ions, which is mediated by the cyanide bridges.[12]

Table 2. Electrochemical Data for $\mathbf{1}^{4-}$−$\mathbf{3}^{4-}$ and Related Mononuclear Fragments

		$E_{1/2}$/V (ΔE_p/mV)[a]	
	solvent	Ru(II/III)	Cr(III/II)
$\mathbf{1}^{4-}$	CH_3CN	+1.03 (80)	−1.79[b]
	MeOH	+1.02 (100)	na
	H_2O	+0.87 (70)	−1.46[b]
$\mathbf{2}^{4-}$	CH_3CN	+0.80 (90)	−1.81[b]
	MeOH	+0.75 (110)	na
	H_2O	+0.62 (70)	−1.44[b]
$\mathbf{3}^{4-}$	CH_3CN	+0.28 (80)	−1.84[b]
	MeOH	+0.20 (70)	na
	H_2O	+0.18 (100)	−1.48[b]
$[Ru(py)_4(CN)_2]$[90]	CH_3CN	+0.80 (90)	
$[Ru(MeOpy)_4(CN)_2]$[86]	CH_3CN	+0.67 (70)	
$[Ru(DMAP)_4(CN)_2]$[24]	CH_3CN	+0.26 (70)	
$[Cr(CN)_6]^{3-}$[44]	H_2O		−1.39[b]

[a]0.1 M [TBA]PF_6 used as electrolyte. na: not available in the solvent electrochemical window. [b]Irreversible.

UV−Vis Spectroelectrochemistry. Figure 3 presents the absorption spectra of $\mathbf{1}^{4-}$−$\mathbf{3}^{4-}$ (black curves), and Table 3 summarizes the spectroscopic data. Two different absorptions are observed for each trimetallic complex in the 300−800 nm region. The high-energy transitions are assigned to dπ(Ru) → π*(L) MLCT charge transfers, with maxima ranging from 340 to 360 nm. These values are comparable to those seen for $[Ru(L)_4(CN)_2]$ in acetonitrile (330−370 nm)[9,24,86] and are blue-shifted with respect to the dπ(Ru) → π*(bpy) absorptions present in {Ru(bpy)$_2$} complexes.[77] A more extended conjugation in bipyridine than in pyridine results in a π*(bpy) orbital stabilization.

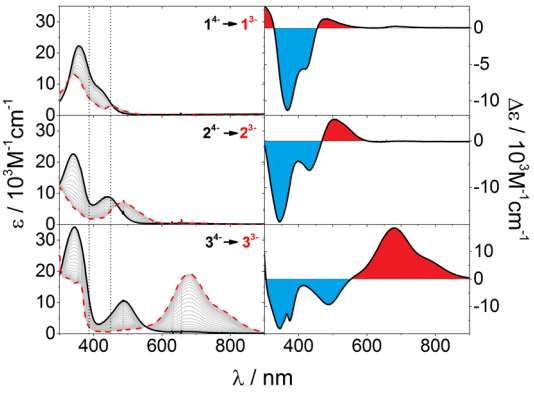

Figure 3. Absorption spectra in methanol: (left panels, black curves) $\mathbf{1}^{4-}$ (top), $\mathbf{2}^{4-}$ (center), and $\mathbf{3}^{4-}$ (bottom); (left panels, red dashed curves) $\mathbf{1}^{3-}$ (top), $\mathbf{2}^{3-}$ (center), and $\mathbf{3}^{3-}$ (bottom). Gray lines indicate spectral evolution throughout the course of the one-electron oxidation. Please note that the dotted lines at 387 and 450 nm represent the laser excitation used in transient absorption experiments. (right panels) Differential absorption spectra reflecting the oxidative process.

No clear trend is seen for the MLCT bands upon pyridine substitution. This is in line with the strong donor character of DMAP, which is, however, compensated by the higher energy of its π*orbitals. The low-energy bands show a clear trend: a shift to the red is observed as the basicity of the substituted pyridine increases. Even here, a bathochromic shift evolves when the solvent acceptor number increases (Table 3). Their energies correlate well with the differences between the ruthenium oxidation and the chromium reduction (Figure S3). This behavior is analogous to that observed in closely related {Fe-Ru-Fe} complexes;[12] hence, these bands are ascribed to dπ(Ru) → dπ(Cr) MM′CT transitions.

One-electron oxidations of $\mathbf{1}^{4-}$−$\mathbf{3}^{4-}$ were studied by spectroelectrochemical means. The left panels of Figure 3 show the spectral evolution during the electrochemical oxidation of $\mathbf{1}^{4-}$−$\mathbf{3}^{4-}$. Both MLCT and MM′CT absorption bands disappear as the Ru(II) depletion occurs. Concomitantly, π(L) → dπ(Ru) LMCT bands develop with maxima at 340/455, 487, and 679 nm for L = py, MeOpy, DMAP, respectively. These signals red-shift as a consequence of increasing the electron donor character of the pyridinic ligands. Very similar LMCT bands are observed for *trans*-$[Ru(L)_4(CN)_2]^+$.[86] Table 3 gathers the spectral data for the one-electron-oxidized trimetallic and monometallic complexes.

In the right panels of Figure 3 the differential absorption spectra upon oxidation are displayed. These are useful to interpret some aspects of transient absorption changes seen upon, for example, charge separation (vide infra). To get a better understanding of the differential absorption spectra regarding the MLCT and MM′CT excited states, pyridinic ligands or chromium centers, respectively, should be studied under reductive conditions. Unfortunately, reductive chemistry of $\mathbf{1}^{4-}$−$\mathbf{3}^{4-}$ is chromium-centered and irreversible (vide supra) and precluded spectroelectrochemical identification of the one-electron-reduced complexes.

Steady-State Photophysics. $\mathbf{1}^{4-}$−$\mathbf{3}^{4-}$ were found to emit in acetonitrile and methanol at room temperature. Their excitation and emission spectra are shown in Figure 4. The emission maxima are around 810−820 nm with lifetimes that

DOI: 10.1021/acs.inorgchem.7b02799
Inorg. Chem. XXXX, XXX, XXX−XXX

Table 3. Spectroscopic Data for 1^{4-}−3^{4-} and Related Mononuclear Fragments as Well as Their One-Electron-Oxidized Forms in Different Solvents

		λ_{max}/nm ($\varepsilon_{max}/10^3$ M^{-1} cm^{-1})		
	solvent	MLCT	MM′CT	LMCT
1^{4-}	CH_3CN	367 (27.2)	nd[a]	
	MeOH	358 (22.2)	420 (8.6)	
	H_2O	347 (21.0)	463 (9.6)	
1^{3-}	MeOH			340 (13.0)
				455 (3.1)
2^{4-}	CH_3CN	355 (23.0)	nd[a]	
	MeOH	341 (21.6)	440 (8.9)	
	H_2O	332 (21.4)	486 (9.8)	
2^{3-}	MeOH			487 (7.2)
3^{4-}	CH_3CN	352 (31.8)	425 (9.5) sh	
	MeOH	345 (35.0)	490 (10.5)	
	H_2O	336 (39.0)	538 (11.6)	
3^{3-}	MeOH			679 (19.3)
				790 (6.9) sh
$[Ru(py)_4(CN)_2]$[90]	CH_3CN	374 (22.5)		
$[Ru(py)_4(CN)_2]^+$[86]	CH_3CN			380 (2.1)
				470 (0.7)
$[Ru(MeOpy)_4(CN)_2]$[86]	CH_3CN	352 (20.5)		
$[Ru(MeOpy)_4(CN)_2]^+$[86]	CH_3CN			400 (2.5) sh
				451 (8.6)
				505 (3.0) sh
$[Ru(DMAP)_4(CN)_2]$[24]	CH_3CN	332 (16.3)		
$[Ru(DMAP)_4(CN)_2]^+$[24]	CH_3CN			614 (16.0)

[a]Not determined, masked by the MLCT absorption.

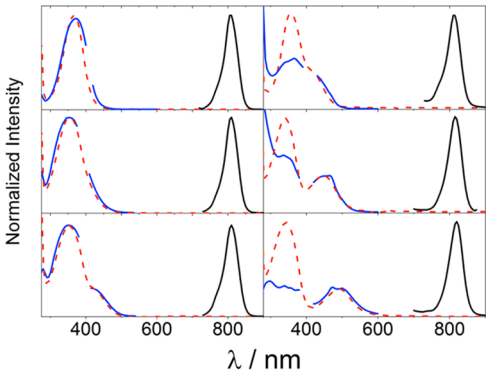

Figure 4. Emission (black solid lines), excitation (blue solid lines), and absorption (dashed red lines) spectra of 1^{4-} (top), 2^{4-} (center), and 3^{4-} (bottom) in acetonitrile (left) and methanol (right).

fall on the microsecond time scale (Table 4).[93] Similar to the case for {Cr-Ru-Cr} compounds bearing the hexacyanidochromate luminophore,[45] no appreciable changes were observed in nondeaerated solutions. Altogether, we conclude that the emission originates from a Cr d−d state.[33,44,94] In acetonitrile, the excitation spectra of compounds 1^{4-}−3^{4-} perfectly match their absorption spectra (Figure 4, left panel), corroborating an effective energy transfer from the $Ru^{III}(L^{-})$ MLCT excited state to the Cr-centered emissive state. This behavior is analogous to that observed in $[(NC)_5Cr(\mu\text{-}CN)Ru(bpy)_2(\mu\text{-}NC)Cr(CN)_5]^{4-}$ (bpy = 2,2′-bipyridine), where the $\{Ru(bpy)_2\}$ fragment acts as the energy donor and the energy transfer efficiency is 100% (η_{ET} = 1).[44] In 1^{4-}−3^{4-}, the energy transfer proceeds with 10−20% efficiency in acetonitrile (see the Experimental Section). Thermal population of closely lying Ru d−d states upon MLCT light absorption is a possible bottleneck. It is even more likely to take place in energetically higher MLCT states, such as those of $\{Ru(py)_4\}$, where it is

Table 4. Photophysical Data for Complexes 1^{4-}−3^{4-} in Argon-Saturated Acetonitrile and Methanol at Room Temperature

				$10^{-4}\varphi_{em}$ (η_{ET})	
	solvent	λ_{em}/nm	$\tau_{MC}/\mu s$	λ_{exc} 390 nm	λ_{exc} 460 nm
$[Cr(CN)_6]^{3-}$	acetonitrile	800	280	18.0 (0.5[44])	
1^{4-}		808	510	8.5 (0.1)	
2^{4-}		808	320	9.6 (0.2)	
3^{4-}		810	370	7.8 (0.2)	
$[Cr(CN)_6]^{3-}$	methanol	802	4.7	2.3 (0.5[44])	
1^{4-}		815	3.1 (8.5)[a]	0.7 (0.2)	4.8 (1)
2^{4-}		815	3.7 (9.6)[a]	1.4 (0.5)	7.6 (1)
3^{4-}		820	1.3 (2.7)[a]	0.5 (0.4)	3.5 (1)

[a]Emission lifetime upon 350 nm excitation (transient absorption lifetime upon 387 nm excitation).

DOI: 10.1021/acs.inorgchem.7b02799
Inorg. Chem. XXXX, XXX, XXX−XXX

expected to be downhill. In {Ru(bpy)$_2$}, Ru d−d state population is usually an uphill process.[77] Hence, the overall energy transfer efficiencies are expected to be lower in {Ru(py)$_4$}-based complexes such as $\mathbf{1}^{4-}$−$\mathbf{3}^{4-}$ than in {Ru(bpy)$_2$}-based analogues. To reach a better overlap with the solar spectrum and render Ru-centered d−d states states more difficult to populate, the next step would be to tune the electronic structure and red-shift the absorption spectra. As a matter of fact, this has already been addressed by variations of the pyridinic rings to extend the overall conjugation.[13]

For $[(NC)_5Cr(\mu\text{-}CN)Ru(bpy)_2(\mu\text{-}NC)Cr(CN)_5]^{4-}$ in DMF,[44] as well as $\mathbf{1}^{4-}$−$\mathbf{3}^{4-}$ in acetonitrile, sensitization by MM′CT states is elusive due to spectral overlap with the more intense MLCT absorptions. This is generally the case for ruthenium polypyridines, and thus, not many reports on MM′CT sensitization have been published. Indelli and co-workers elegantly overcame this bottleneck in the form of {Cr-Ru-Cr},[45] where a Ru fragment transparent in the visible region was covalently linked to {Cr(cyclam)}, and they corroborated energy transfer efficiencies of 100% from the MM′CT states to Cr-centered d−d states.

In $\mathbf{1}^{4-}$−$\mathbf{3}^{4-}$, high energy MLCT bands of {Ru(py)$_4$} and the solvent control over the energy of the electronic states of hexacyanidometallates are combined. This results in a clear separation of MLCT and MM′CT absorptions in methanol. In this solvent, the excitation spectra match the MM′CT absorptions. In the region of MLCT transitions, the excitation spectra lose intensity in comparison with the absorption profiles. This might be related to thermal population of Ru d−d states, which is more pronounced from MLCT than from MM′CT states. Table 4 pinpoints higher emission quantum yields upon 460 nm (MM′CT) rather than 390 nm (MLCT) illumination. It is important to note that the emission wavelengths of $\mathbf{1}^{4-}$−$\mathbf{3}^{4-}$ in methanol under MM′CT illumination are very similar, despite different MM′CT state energies. These results allow us to rule out major contributions from MM′CT emission, which is in stark contrast to {Cr-Ru-Cr} complexes reported by Endicott and co-workers.[95,96]

η_{ET} is smaller when the processes start at MLCT rather than MM′CT states. This stems from the fundamental differences between these states. MLCT donor states are subject to a depopulation via closely lying Ru-centered d−d states; this lowers the energy transfer efficiency. Substitution on the para positions of the L ligands exerts no observable influence on the energy transfer efficiencies. Both Förster and Dexter mechanisms may be operative in these intramolecular energy transfer processes, starting either in a MLCT or in a MM′CT donor state. A Coulombic mechanism can not be ruled out because of the presence of several metal centers with high spin multiplicity in the excited states.[97] Several spin states should be considered, which may participate in a Förster mechanism by obeying the total spin conservation.[98] As our energy-donating {Ru(L)$_4$} fragments are nonemissive in the absence of any energy acceptor, estimations of the energy transfer rate constant using Förster's model are not possible. Notably, exchange pathways have been observed for similar systems.[44,46] They may also contribute in $\mathbf{1}^{4-}$−$\mathbf{3}^{4-}$ due to the rather short cyanide bridge (the Ru−Cr crystallographic distance is ∼5 Å) and the efficient electronic communication.[99,100]

Transient Absorption Spectroscopy. Transient absorption spectra were recorded in methanol on both the picosecond and microsecond time scales to gather insight into the sensitization processes evolving from {Ru(L)$_4$} in $\mathbf{1}^{4-}$−$\mathbf{3}^{4-}$. Either 450 or 387 nm excitation was used to evaluate the role of MM′CT and MLCT states as energy donors, respectively.

On the microsecond time scale, $\mathbf{1}^{4-}$−$\mathbf{3}^{4-}$ give rise to differential spectra, which are independent of the excitation wavelength (Figure 5) and which decay monoexponentially to

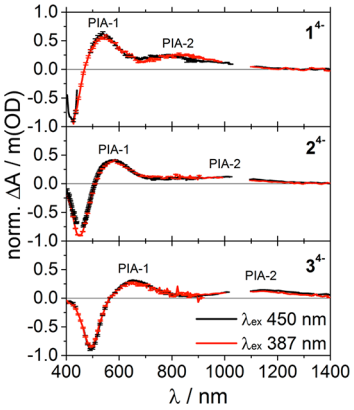

Figure 5. Species associated difference spectra (SADS) obtained by global analysis using a single-state model for $\mathbf{1}^{4-}$ (top), $\mathbf{2}^{4-}$ (center), and $\mathbf{3}^{4-}$ (bottom) in MeOH, upon 450 nm (black curves) and 387 nm (red curves) excitation, on the microsecond time scale.

zero (Figures S4−S6). A common state is finally populated under 387 and 450 nm illumination, whose depopulation goes hand in hand with ground-state recovery. For $\mathbf{1}^{4-}$, a single bleaching at 425 nm (2.92 eV) and two photoinduced absorptions at 540 nm (2.30 eV, PIA-1) and 820 nm (1.51 eV, PIA-2) are noted. From global analysis of the 450 nm excitation data a time constant of 6.4 μs is concluded (Figure S6 and Table 5). The same pattern is observed for $\mathbf{2}^{4-}$, with a 450 nm bleaching (2.76 eV) and 580 and 950 nm absorptions (2.14 and 1.31 eV), which decay with a time constant of 9.0 μs. In the case of $\mathbf{3}^{4-}$, the bleaching is at 490 nm (2.53 eV), while the maxima are at 650 and 1150 nm (1.91 and 1.08 eV). Overall, they decay in 3.0 μs. Upon 387 nm excitation, very similar results are obtained (Table 5). On the basis of the lifetimes of these states we label them as emissive Cr* states, whose differential absorption spectra are discussed below.

Picosecond experiments provided information about the population of the emissive Cr* states.[101] On this time scale, the dynamics depend on the excitation wavelength and both experiments are analyzed separately. Upon excitation at 450 nm, negative signals in the blue part of the spectrum appear, and afterward broad photoinduced absorptions evolve in the red part (Figure S7). According to global analysis, only one exponential process in the picosecond time scale takes place.[84,85] The time constants are given in Table 5, and the corresponding SADS$_{450\ nm}$ are shown in Figure 6. As inferred from the ground-state absorption spectra (Figure 3), excitation at 450 nm of $\mathbf{1}^{4-}$ and $\mathbf{2}^{4-}$ leads to an initial population of MM′CT states. The differential spectra of MM′CT states include a negative signal, which mirrors the MM′CT ground-state absorption, and very weak absorptions in the red part (SADS1$_{450\ nm}$, black curves in the left panel of Figure 6). These features evolve with lifetimes of 1.4 ps for $\mathbf{1}^{4-}$ and 0.6 ps for $\mathbf{2}^{4-}$. The resulting spectra (SADS2$_{450\ nm}$, blue curves in the left panel of Figure 6) are in sound agreement with those obtained in the microsecond experiments, which leads us to assign them as Cr* states. Our interpretation implies that the picosecond lifetimes account for the energy transfer.

DOI: 10.1021/acs.inorgchem.7b02799
Inorg. Chem. XXXX, XXX, XXX−XXX

Table 5. Time Constants Extracted from Global and Target Analyses of Transient Absorption Experiments for Complexes 1^{4-}–3^{4-}, Using the Target Models Depicted in Figure 6[a]

compound	pump/nm	τ_1/ps (k_1/ps^{-1})	τ_2/ps (k_2/ps^{-1})	τ_3/μs (k_3/μs^{-1})
1^{4-}	450		1.4 (0.72 ± 0.01)	6.4 (0.156 ± 0.001)
	387	6.8 (0.15 ± 0.03)	57 (1.76 ± 0.07) × 10^{-2}	8.5 (0.118 ± 0.001)
2^{4-}	450		0.6 (1.65 ± 0.01)	9.0 (0.111 ± 0.001)
	387	0.6 (1.70 ± 0.03)	15 (6.9 ± 0.2) × 10^{-2}	9.6 (0.104 ± 0.001)
3^{4-}	450	nd	nd	3.0 (0.338 ± 0.001)
	387	nd	nd	2.7 (0.368 ± 0.007)

[a]nd: not determined (see ref 101).

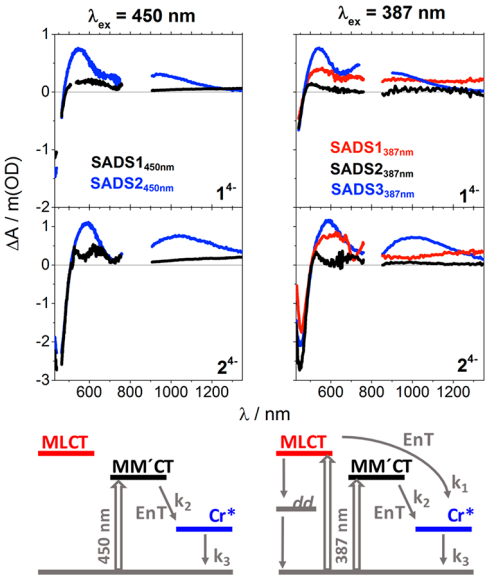

Figure 6. Species associated difference spectra (SADS) for 1^{4-} (top) and 2^{4-} (center) in MeOH upon 450 nm (left) and 387 nm (right) excitation on the picosecond time scale, obtained by target analysis using the model depicted at the bottom.

In 387 nm excitation experiments with 1^{4-} and 2^{4-}, a bleaching as a mirror image of the MM′CT ground-state absorption and positive signals in the red part of the spectrum are observed (Figure S8). Global fitting of the data renders three spectrally active components. Please note that the 387 nm excitation is in near resonance with both MLCT and MM′CT ground state absorptions (dotted lines in Figure 3). Initially, both excited states are populated simultaneously, which required target analysis to resolve the different states involved. In the proposed model, two initially populated excited states ($SADS1_{387\,nm}$ and $SADS2_{387\,nm}$), which transform with two different time constants into a third, long-lived excited state ($SADS3_{387\,nm}$), are included. The time constants are given in Table 5, and the corresponding $SADS_{387\,nm}$ are shown in Figure 6. $SADS1_{387\,nm}$ and $SADS2_{387\,nm}$ show a bleached MM′CT ground-state absorption, in combination with red-shifted photoinduced absorptions in the case of $SADS1_{387\,nm}$. Importantly, $SADS2_{387\,nm}$ resembles $SADS1_{450\,nm}$. Thus, we assign $SADS1_{387\,nm}$ and $SADS2_{387\,nm}$ to the MLCT and MM′CT excited states, respectively, which both populate $SADS3_{387\,nm}$. The differential absorption of the later resembles that obtained in the microsecond time scale and is therefore assigned to the emissive Cr* state.

DISCUSSION

Spectral Profiles and Nature of the Chromium-Centered Emissive States. For 1^{4-}–3^{4-}, both the emission and the transient absorption spectra give rise to monoexponential decays on the microsecond time scale. Therefore, we assign the observed emission to a chromium-centered ^{2}E excited state. Their lifetimes are comparable to those of $[Cr(CN)_6]^{3-}$ and pentacyanidochromate(III) complexes.[94] The microsecond-lived transients (Figure 5) of 1^{4-}–3^{4-} feature a pattern very similar to what is observed for other {Cr-Ru-Cr} complexes:[45,46] namely, bleaching and two positive signals (PIA-1 and PIA-2). The negative signals mirror the MM′CT ground state maxima at 425, 450, and 490 nm (2.92, 2.76, and 2.53 eV) for 1^{4-}–3^{4-}, respectively. The energetic difference between these negative signals and each PIA-2 (at 820 nm or

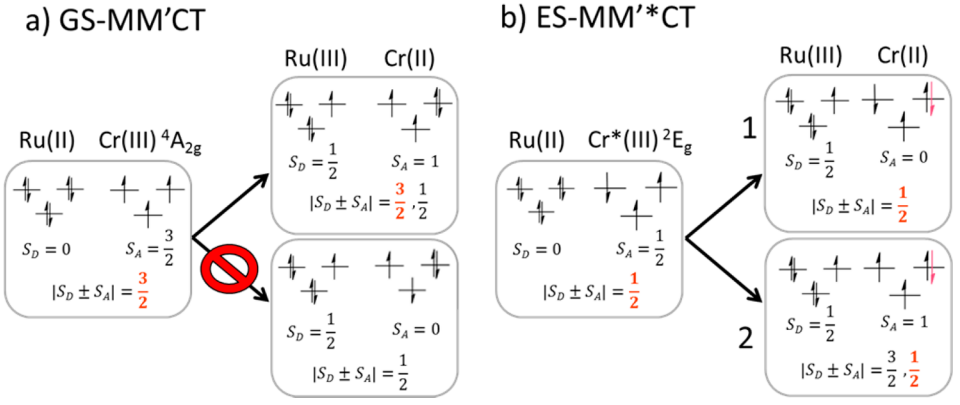

Figure 7. Electronic configurations of the initial and final states potentially involved in (a) ground- or (b) excited-state metal–metal′ charge transfer transitions. Only those orbitals parallel to the intermetallic axis have been considered to appreciably contribute to the observed charge transfer intensity.

DOI: 10.1021/acs.inorgchem.7b02799
Inorg. Chem. XXXX, XXX, XXX–XXX

1.51 eV for L = py, at 950 nm or 1.31 eV for L = MeOpy, and at 1150 nm or 1.08 eV for L = DMAP) is nearly constant and consistent with the estimated energy of the emissive Cr* states (1.52 eV). In other words, we assign the PIA-2 as MM′*CT transitions.[44−46] PIA-1 at 540 nm (2.30 eV) for L = py, at 580 nm (2.14 eV) for L = MeOpy, and at 650 nm (1.91 eV) for L = DMAP, respectively, shows a similar dependence on the ligand. They shift to lower energies on going from py to DMAP, leading us to locate the orbital origin of PIA-1 transitions on the ruthenium center. From the fact that adding some water produces further red shifts, we conclude that the acceptor orbital is located at hexacyanidochromate.[12,102] These signals are accordingly ascribed to MM'*CT transitions.

Two separated MM′*CT transitions, which correspond to the Cr* ^{2}E excited state, are rationalizable in terms of the electronic configuration of Cr*(III). Metal to metal charge transfer from Ru(II) to Cr*(III) may hypothetically result in two different MM′CT states, which obey spin conservation through transitions #1 and #2 in Figure 7b.[103] Transition #2 leads to a final state, which is identical with that corresponding to the GS-MM′CT. Considering the energetics, we conclude that PIA-2 generates this particular configuration. PIA-1 results in configuration #1 in Figure 7b.

450 nm Excitation: MM′CT States as Energy Donors. Upon 450 nm excitation, the initially populated MM′CT excited state is formally described as {Ru(III)-Cr(II)}. Ru(III) is responsible for the bleaching of the MM′CT ground state absorption and for the weak photoinduced π(L) → dπ(Ru) LMCT transition observed for $SADS1_{450\,nm}$. These features are in sound agreement with those obtained from oxidative spectroelectrochemistry (Figure 3). Energy transfer lifetimes of 1.4 and 0.6 ps for L = py and L = MeOpy, respectively, are consistent with a unit efficiency determined in steady-state experiments.

387 nm Excitation: MLCT/MM′CT Excited States as Energy Donors. Upon 387 nm excitation, the initially populated MLCT excited state is formally described as {Ru(III)(L$^{\bullet-}$)}. These and the MM′CT states share a common {Ru(III)}, but the location of the excited electron differs. It resides either on a ligand (MLCT) or on a chromium ion (MM′CT). Accordingly, $SADS1_{387\,nm}$ presents enhanced photoinduced absorptions at λ >550 nm, which we ascribe to the L radical anion as part of the MLCT excited state and which matches the reductive spectroelectrochemical response of these ligands.[8] $SADS3_{387\,nm}$ matches the microsecond spectra, confirming its assignment as a Cr* state. Any efforts to include Ru d−d states in the decay model were unsuccessful. This is probably a consequence of depopulation, which is faster than the generation of such states, impeding an observable buildup.

The energy transfer processes from $MM'CT_{387\,nm}$ states are slower than those from the $MM'CT_{450\,nm}$ states. However, it should be noted that their SADS differ slightly, and this suggests different electronic configurations for both MM′CT states: i.e., the hole is located in a different orbital of the Ru(III) ion. This would explain the different energy transfer constants. It is interesting to note that the energy transfer from either state is faster when L is a better donor, that is, when the metal centers are more strongly coupled. This reflects an important prerequisite for a Dexter mechanism for an energy transfer involving Cr* states. Similar values are found in analogous complexes. Using ruthenium polypyridine complexes as donors, the phenomenon takes around 4 ps.[91,104]

Overall, the experiments presented here document {Ru(py)$_4$}-sensitized energy transfer processes. The only limitation is the undesired population of Ru d−d states under high-energy excitation, which reduces the MLCT lifetimes and, in turn, limits the utilization of these chromophores to fast, short-range energy transfers. {Ru(py)$_4$} fragments with acceptor substituents in the 4-position, which shift the MLCT to the red and, in turn, disfavor thermal population of Ru d−d states, are a potential solution. At the same time, these ligand modifications provide the means for a better light harvesting across the solar spectrum.

CONCLUSION

We prepared *trans*-[Ru(L)$_4${(μNC)Cr(CN)$_5$}$_2$]$^{4-}$ trimetallic complexes, whose structures were confirmed by X-ray diffraction. Their electrochemical properties and UV−vis absorption spectra were determined and corroborated the expected dependence on the solvent acceptor character and the L donor abilities. Irradiation of $\mathbf{1}^{4-}$−$\mathbf{3}^{4-}$ into either their MLCT or MM′CT absorptions resulted in energy transfer processes to the emissive Cr* state. To the best of our knowledge, this is the first report regarding a {Ru(py)$_4$}-sensitized energy transfer process. Energy transfer efficiencies are of the same order of magnitude as in the {Cr-Ru(bpy)$_2$-Cr} analogues. From this point of view, {Ru(py)$_4$} is a promising short-range chromophore fragment employable as a photosensitizer in supramolecular systems. However, population of Ru d−d states, which is detrimental for energy or charge extraction from these fragments and could even lead to photodecomposition, is still a drawback. Currently, we are exploring substitutions on the pyridinic ligands of {Ru(py)$_4$} to create a large energy gap between the MLCT and d−d states and, in turn, to hinder the d−d state population. In addition, this would be helpful in terms of realizing a better match with the solar spectrum and, in turn, rendering it a better sunlight harvester.

ASSOCIATED CONTENT

Supporting Information

The Supporting Information is available free of charge on the ACS Publications website at DOI: 10.1021/acs.inorgchem.7b02799.

Crystallographic data for $\mathbf{2(PPh_4)_4}$ and $\mathbf{3(PPh_4)_4}$, cyclic voltammograms, correlation between the energy of the MM′CT band and the difference between the reduction potentials of ruthenium and chromium metal centers in water, and transient absorption measurements in the microsecond and picosecond time scales (PDF)

Accession Codes

CCDC 1408010−1408011 contain the supplementary crystallographic data for this paper. These data can be obtained free of charge via www.ccdc.cam.ac.uk/data_request/cif, or by emailing data_request@ccdc.cam.ac.uk, or by contacting The Cambridge Crystallographic Data Centre, 12 Union Road, Cambridge CB2 1EZ, UK; fax: +44 1223 336033.

AUTHOR INFORMATION

Corresponding Authors

*E-mail for A.C.: ale.cadranel@fau.de.
*E-mail for J.H.H.: jhodak@qi.fcen.uba.ar.

DOI: 10.1021/acs.inorgchem.7b02799
Inorg. Chem. XXXX, XXX, XXX−XXX

ORCID

Alejandro Cadranel: 0000-0002-6597-4397
Pablo Alborés: 0000-0002-6181-4521
Luis M. Baraldo: 0000-0003-0666-5540
Dirk M. Guldi: 0000-0002-3960-1765

Notes

The authors declare no competing financial interest.

■ ACKNOWLEDGMENTS

The authors thank Dr. Eva Rentschler for providing access to XRD measurements. The authors acknowledge the University of Buenos Aires (UBACYT Q643), the Consejo Nacional de Investigaciones Cintíficas y Técnicas (CONICET), and the Agencia Nacional de Promoción Científica y Tecnológica (PICT 2012-2041) for funding. J.H.H., L.M.B., and P.A. are members of the scientific staff of CONICET; P.S.O. is a doctoral fellow of the same institution. A.C. is grateful to CONICET, DAAD, and Ministerio de Educación de la Nación Argentina for postdoctoral fellowships and to ALN for supporting interventions.

■ REFERENCES

(1) Barigelletti, F.; Flamigni, L. Photoactive Molecular Wires Based on Metal Complexes. *Chem. Soc. Rev.* **2000**, *29*, 1−12.
(2) Sun, L.; Hammarström, L.; Åkermark, B.; Styring, S. Towards Artificial Photosynthesis: Ruthenium−manganese Chemistry for Energy Production. *Chem. Soc. Rev.* **2001**, *30*, 36−49.
(3) Balzani, V.; Juris, A. Photochemistry and Photophysics of Ru (II) Polypyridine Complexes in the Bologna Group. From Early Studies to Recent Developments. *Coord. Chem. Rev.* **2001**, *211*, 97−115.
(4) Huynh, M. H. V.; Dattelbaum, D. M.; Meyer, T. J. Exited State Electron and Energy Transfer in Molecular Assemblies. *Coord. Chem. Rev.* **2005**, *249*, 457−483.
(5) Hagfeldt, A.; Boschloo, G.; Sun, L.; Kloo, L.; Pettersson, H. Dye-Sensitized Solar Cells. *Chem. Rev.* **2010**, *110*, 6595−6663.
(6) Grätzel, M. Conversion of Sunlight to Electric Power by Nanocrystalline Dye-Sensitized Solar Cells. *J. Photochem. Photobiol., A* **2004**, *164*, 3−14.
(7) Polo, A. S.; Itokazu, M. K.; Murakami Iha, N. Y. Metal Complex Sensitizers in Dye-Sensitized Solar Cells. *Coord. Chem. Rev.* **2004**, *248*, 1343−1361.
(8) Cadranel, A.; Pieslinger, G. E.; Tongying, P.; Kuno, M. K.; Baraldo, L. M.; Hodak, J. H. Spectroscopic Signatures of Ligand Field States in $\{Ru^{II}(imine)\}$ Complexes. *Dalton Trans.* **2016**, *45*, 5464−5475.
(9) Coe, B. J.; Meyer, T. J.; White, P. S. Cyano-Bridged Complexes of Trans-Tetrakis(pyridine)ruthenium(II). *Inorg. Chem.* **1995**, *34*, 3600−3609.
(10) Naka, K.; Kobayashi, A.; Chujo, Y. Synthesis of a Star-Shaped Polymer via Coordination of Ester-Linked Pyridyl-Terminated Poly(oxyethylene) with Ru(II). *Macromol. Rapid Commun.* **1997**, *18*, 1025−1032.
(11) Sheng, T.; Vahrenkamp, H. Long Range Metal-Metal Interactions Along Fe−NC−Ru−CN−Fe Chains. *Eur. J. Inorg. Chem.* **2004**, *2004*, 1198−1203.
(12) Alborés, P.; Slep, L. D.; Weyhermüller, T.; Baraldo, L. L. M. Fine Tuning of the Electronic Coupling between Metal Centers in Cyano-Bridged Mixed-Valent Trinuclear Complexes. *Inorg. Chem.* **2004**, *43*, 6762−6773.
(13) Cadranel, A.; Hodak, J. H. Four Chromophores in One Building Block: Synthesis, Structure and Characterization of Trans-$[Ru(MQ)_4Cl_2]^{4+}$ and Trans-$[Ru(4,4'\text{-bpy})_4Cl_2]$ (MQ+ = N-Methyl-4,4'-Bipyridinium, Bpy = Bipyridine. *J. Coord. Chem.* **2015**, *68*, 1452−1464.
(14) Pieslinger, G. E.; Aramburu-Trošelj, B. M.; Cadranel, A.; Baraldo, L. M. Influence of the Electronic Configuration in the Properties of d(6)-d(5) Mixed-Valence Complexes. *Inorg. Chem.* **2014**, *53*, 8221−8229.
(15) Marcolongo, J. P.; Weyhermüller, T.; Slep, L. D. Exploring the Photo-Stability of the $\{Ru(py)_4\}^{2+}$ Fragment. *Inorg. Chim. Acta* **2015**, *429*, 174−182.
(16) De Candia, A. G.; Singh, P.; Kaim, W.; Slep, L. D. All-Trans-$[ClRu^{II}(py)_4(NC)Ru^{II}(py)_4(CN)Ru^{II}(py)_4(NO)](PF_6)_4$: A Redox-Active 2-Donor/1-Acceptor System Based on the Electrophilic $\{RuNO\}^6$ Motif. *Inorg. Chem.* **2009**, *48*, 565−573.
(17) Roncaroli, F.; Baraldo, L. M.; Slep, L. D.; Olabe, J. A. Metallonitrosyl Fragment as Electron Acceptor: Intramolecular Charge Transfer, Long Range Electronic Coupling, and Electrophilic Reactivity in the Trans-$[NCRu(py)_4(CN)Ru(py)_4NO]^{3+}$ Ion. *Inorg. Chem.* **2002**, *41*, 1930−1939.
(18) Gajardo, F.; Leiva, A. M.; Loeb, B.; Delgadillo, A.; Stromberg, J. R.; Meyer, G. J. Interfacial Electron Transfer on TiO_2 Sensitized with an Axially Anchored Trans Tetradentate Ru(II) Compound. *Inorg. Chim. Acta* **2008**, *361*, 613−619.
(19) Nikol'Skii, A. B.; Varshavsky, Y. S.; Cherkasova, T. G.; Podkorytov, I. S.; Gindin, V. A. Interfragment Transmission of Electronic Effects of π-Acceptor Ligands in Heterometallic Triad Complexes with Trans-$[Ru(Py)_4(CN)_2]$ as a Central Unit. *Russ. Chem. Bull.* **2012**, *61*, 813−820.
(20) Macatangay, A. V.; Endicott, J. F. Vibronic Coupling in Dicyano-Complex-Bridged Mixed-Valence Complexes. Relaxation of Vibronic Constraints in Systems with Degenerate Bridging-Ligand and Electron-Transfer Excited States. *Inorg. Chem.* **2000**, *39*, 437−446.
(21) Desjardins, P.; Yap, G. P. A.; Crutchley, R. J. Tetrakis(Pyridine)Ruthenium Trans Complexes of Phenylcyanamide Ligands: Crystallography, Electronic Absorption Spectroscopy, and Cyclic Voltammetry. *Inorg. Chem.* **1999**, *38*, 5901−5905.
(22) Biancardo, M.; Schwab, P. F. H.; Argazzi, R.; Bignozzi, C. A. Electrochromic Devices Based on Binuclear Mixed Valence Compounds Adsorbed on Nanocrystalline Semiconductors. *Inorg. Chem.* **2003**, *42*, 3966−3968.
(23) Sizova, O.; Ivanova, N.; Baranovskii, V.; Panin, A.; Nikol'Skii, A. Chemistry of Binuclear Bridged Platinum Metal Complexes: VII. Quantum-Chemical Simulation of "Molecular Assembling": Series $[Ru(CN)_2(py)_4]$, $[Cl(py)_4Ru\text{-}NC\text{-}Ru(py)_4CN]^+$, $[Cl(py)_4Ru\text{-}NC\text{-}Ru(py)_4\text{-}CN\text{-}Ru(py)_4Cl]^{2+}$. *Russ. J. Gen. Chem.* **2000**, *70*, 823−827.
(24) Pieslinger, G. E.; Alborés, P.; Slep, L. D.; Baraldo, L. M. Class III Delocalization in a Cyanide-Bridged Trimetallic Mixed-Valence Complex. *Angew. Chem., Int. Ed.* **2014**, *53*, 1293−1296.
(25) Endicott, J. F.; Chen, Y.-J. Electronic Coupling between Metal Ions in Cyanide-Bridged Ground State and Excited State Mixed Valence Complexes. *Coord. Chem. Rev.* **2013**, *257*, 1676−1698.
(26) Scandola, F.; Argazzi, R.; Bignozzi, C. A.; Chiorboli, C.; Indelli, M. T.; Rampi, M. A. Electronic Coupling between Remote Metal Centers in Cyanobridged Polynuclear Complexes. *Coord. Chem. Rev.* **1993**, *125*, 283−292.
(27) Bignozzi, C. A.; Argazzi, R.; Garcia, C. G.; Scandola, F.; Schoonover, J. R.; Meyer, T. J. Long Range Energy Transfer in Oligomeric Metal Complex Assemblies. *J. Am. Chem. Soc.* **1992**, *114*, 8727−8729.
(28) Wagenknecht, P. S.; Ford, P. C. Metal Centered Ligand Field Excited States: Their Roles in the Design and Performance of Transition Metal Based Photochemical Molecular Devices. *Coord. Chem. Rev.* **2011**, *255*, 591−616.
(29) Büldt, L. A.; Wenger, O. S. Chromium Complexes for Luminescence, Solar Cells, Photoredox Catalysis, Upconversion, and Phototriggered NO Release. *Chem. Sci.* **2017**, *8*, 7359−7367.
(30) Forster, L. S. Thermal Relaxation in Excited Electronic States of d^3 and d^6 Metal Complexes. *Coord. Chem. Rev.* **2002**, *227*, 59−92.
(31) Keith DeArmond, M.; Carlin, C. M. Multiple State Emission and Related Phenomena in Transition Metal Complexes. *Coord. Chem. Rev.* **1981**, *36*, 325−355.
(32) Serpone, N.; Jamieson, M. A. Picosecond Spectroscopy of Transition Metal Complexes. *Coord. Chem. Rev.* **1989**, *93*, 87−153.

DOI: 10.1021/acs.inorgchem.7b02799
Inorg. Chem. XXXX, XXX, XXX−XXX

(33) Forster, L. S. The Photophysics of Chromium(III) Complexes. *Chem. Rev.* **1990**, *90*, 331−353.
(34) Endicott, J. F.; Ramasami, T.; Tamilarasan, R.; Lessard, R. B.; Ryu, C. K.; Brubaker, G. R. Structure and Reactivity of the Metal-Centered Transition Metal Excited States. *Coord. Chem. Rev.* **1987**, *77*, 1−87.
(35) Bolletta, F.; Maestri, M.; Balzanl, V. Efficiency of the Intersystem Crossing from the Lowest Spin-Allowed to the Lowest Spin-Forbidden Excited State of Some Chromium(III) and Ruthenium(II) Complexes. *J. Phys. Chem.* **1976**, *80*, 2499−2503.
(36) Serpone, N.; Jamieson, M. A.; Henry, M. S.; Hoffman, M. Z.; Bolletta, F.; Maestri, M. Excited-State Behavior of Polypyridyl Complexes of Chromium(III). *J. Am. Chem. Soc.* **1979**, *101*, 2907−2916.
(37) Otto, S.; Grabolle, M.; Förster, C.; Kreitner, C.; Resch-Genger, U.; Heinze, K. $[Cr(ddpd)_2]^{3+}$: A Molecular, Water-Soluble, Highly NIR-Emissive Ruby Analogue. *Angew. Chem., Int. Ed.* **2015**, *54*, 11572−11576.
(38) Otto, S.; Nauth, A. M.; Ermilov, E.; Scholz, N.; Friedrich, A.; Resch-Genger, U.; Lochbrunner, S.; Opatz, T.; Heinze, K. Photo-Chromium: Sensitizer for Visible-Light-Induced Oxidative C−H Bond Functionalization-Electron or Energy Transfer? *ChemPhotoChem.* **2017**, *1*, 344−349.
(39) Zare, D.; Doistau, B.; Nozary, H.; Besnard, C.; Guénée, L.; Suffren, Y.; Pelé, A.-L.; Hauser, A.; Piguet, C. Cr III as an Alternative to Ru II in Metallo-Supramolecular Chemistry. *Dalton Trans.* **2017**, *46*, 8992−9009.
(40) Wang, C.; Otto, S.; Dorn, M.; Kreidt, E.; Lebon, J.; Sran, L.; Di Martino-Fumo, P.; Gerhards, M.; Resch-Genger, U.; Seitz, M.; Heinze, K. Deuterated Molecular Ruby with Record Luminescence Quantum Yield. *Angew. Chem., Int. Ed.* **2018**, *57*, 1112−1116.
(41) Barbour, J. C.; Kim, A. J. I.; DeVries, E.; Shaner, S. E.; Lovaasen, B. M. Chromium(III) Bis-Arylterpyridyl Complexes with Enhanced Visible Absorption via Incorporation of Intraligand Charge-Transfer Transitions. *Inorg. Chem.* **2017**, *56*, 8212−8222.
(42) Castelli, F.; Forster, L. S. Multiple Decays of $Cr(CN)_6^{3-}$ Emission in Rigid Glass Solutions. *J. Am. Chem. Soc.* **1973**, *95*, 7223−7226.
(43) Sabbatini, N.; Scandola, M. A.; Balzani, V. Intersystem Crossing Efficiency in the Hexacyanochromate(III) Ion. *J. Phys. Chem.* **1974**, *78*, 541−543.
(44) Bignozzi, C. A.; Indelli, M. T.; Scandola, F. bis(2,2'-bipyridine)ruthenium(II)-Hexacyanochromate (III) Chromophore-Luminophore Complexes. Intramolecular Energy Transfer, Excited-State Intervalence Transfer, and Doublet-Doublet Annihilation. *J. Am. Chem. Soc.* **1989**, *111*, 5192−5198.
(45) Indelli, M. T.; Scandola, F. Excited-State Charge Recombination in a Ru(II)-Cr(III) Polynuclear Complex. *J. Phys. Chem.* **1993**, *97*, 3328−3332.
(46) Bignozzi, C. A.; Bortolini, O.; Chiorboli, C.; Indelli, M. T.; Rampi, M. A.; Scandola, F. Intramolecular Energy Transfer in ruthenium(II)-chromium(III) Chromophore-Luminophore Complexes. $Ru(bpy)_2[Cr(cyclam)(CN)_2]_2^{4+}$. *Inorg. Chem.* **1992**, *31*, 172−177.
(47) Kane-Maguire, N. A. P.; Crippen, W. S.; Miller, P. K. Unusual Photobehavior of Trans -Dicyano(1,4,8,11-tetraazacyclotetradecane)-chromium(III) Perchlorate. *Inorg. Chem.* **1983**, *22*, 696−698.
(48) Ryu, C. K.; Endicott, J. F. Synthesis, Spectroscopy, and Photophysical Behavior of Mixed-Ligand Mono- and Bis(polypyridyl)-chromium(III) Complexes. Examples of Efficient, Thermally Activated Excited-State Relaxation without Back Intersystem Crossing. *Inorg. Chem.* **1988**, *27*, 2203−2214.
(49) Ryu, C. K.; Lessard, R. B.; Lynch, D.; Endicott, J. F. Multiple Channel Nuclear and Electronic Tunneling in the Low-Temperature Decay of the ^2E Excited-State of Chromium(III) Complexes. *J. Phys. Chem.* **1989**, *93*, 1752−1759.
(50) Lessard, R. B.; Endicott, J. F.; Perkovic, M. W.; Ochrymowycz, L. A. Perturbations of the Low-Energy Doublet Excited State of Chromium(III): Competing Heavy-Atom and Macrocyclic Ligand Effects in Thermally Activated Relaxation Pathways. *Inorg. Chem.* **1989**, *28*, 2574−2583.
(51) Bignozzi, C. A.; Chiorboli, C.; Indelli, M. T.; Scandola, F.; Bertolasi, V.; Gilli, G. Molecular Structure and Linkage Isomerism of Cis-$[Ru(bipy)_2$-{trans-$Cr(cyclam)(CN)_2$}$_2]^{4+}$ (Bipy = 2,2'-bipyridine, Cyclam = 1,4,8,11-Tetraazacyclotetradecane). *J. Chem. Soc., Dalton Trans.* **1994**, *0*, 2391−2395.
(52) Lessard, R. B.; Heeg, M. J.; Buranda, T.; Perkovic, M. W.; Schwarz, C. L.; Rudong, Y.; Endicott, J. F. Stereochemical Alterations of ^2E Chromium(III) Excited-State Behavior in Dicyanotetraazacyclotetradecane Complexes. Ground-State X-Ray Crystal Structures, Photophysical Behavior, and Molecular Mechanics Simulations of Stereochemical Effects. *Inorg. Chem.* **1992**, *31*, 3091−3103.
(53) Wagenknecht, P. S.; Hu, C.; Ferguson, D.; Nathan, L. C.; Hancock, R. D.; Whitehead, J. R.; Wright-Garcia, K.; Vagnini, M. T. Effects of Steric Constraint on chromium(III) Complexes of Tetraazamacrocycles, 2. Comparison of the Chemistry and Photobehavior of the Trans-Dichloro- and Trans-Dicyano- Complexes of Cyclam, 1,4-C_2-Cyclam, and 1,11-C_3-Cyclam. *Inorg. Chem.* **2005**, *44*, 9518−9526.
(54) Vagnini, M. T.; Kane-Maguire, N. A. P.; Wagenknecht, P. S. Effects of Steric Constraint on chromium(III) Complexes of Tetraazamacrocycles. 3. Insights into the Temperature-Dependent Radiationless Deactivation of the ^2E_g (Oh) Excited State of Trans-$[Cr(N_4)(CN)_2]^+$ Complexes. *Inorg. Chem.* **2006**, *45*, 3789−3793.
(55) Milos, M.; Hauser, A. Chromium(III)-Trisoxalate, a Versatile Building Block for Luminescent Materials. *J. Lumin.* **2013**, *133*, 15−20.
(56) McDaniel, A. M.; Tseng, H. W.; Damrauer, N. H.; Shores, M. P. Synthesis and Solution Phase Characterization of Strongly Photooxidizing Heteroleptic Cr(III) Tris-Dipyridyl Complexes. *Inorg. Chem.* **2010**, *49*, 7981−7991.
(57) Aboshyan-Sorgho, L.; Besnard, C.; Pattison, P.; Kittilstved, K. R.; Aebischer, A.; Bünzli, J. C. G.; Hauser, A.; Piguet, C. Near-infrared→Visible Light Upconversion in a Molecular Trinuclear D-F-D Complex. *Angew. Chem., Int. Ed.* **2011**, *50*, 4108−4112.
(58) Aboshyan-Sorgho, L.; Cantuel, M.; Petoud, S.; Hauser, A.; Piguet, C. Optical Sensitization and Upconversion in Discrete Polynuclear Chromium-Lanthanide Complexes. *Coord. Chem. Rev.* **2012**, *256*, 1644−1663.
(59) Yoon, T. P.; Ischay, M. A.; Du, J. Visible Light Photocatalysis as a Greener Approach to Photochemical Synthesis. *Nat. Chem.* **2010**, *2*, 527−532.
(60) Narayanam, J. M. R.; Stephenson, C. R. J. Visible Light Photoredox Catalysis: Applications in Organic Synthesis. *Chem. Soc. Rev.* **2011**, *40*, 102−113.
(61) Xuan, J.; Xiao, W. J. Visible-Light Photoredox Catalysis. *Angew. Chem., Int. Ed.* **2012**, *51*, 6828−6838.
(62) Prier, C. K.; Rankic, D. A.; MacMillan, D. W. C. Visible Light Photoredox Catalysis with Transition Metal Complexes: Applications in Organic Synthesis. *Chem. Rev.* **2013**, *113*, 5322−5363.
(63) Beatty, J. W.; Stephenson, C. R. J. Amine Functionalization via Oxidative Photoredox Catalysis: Methodology Development and Complex Molecule Synthesis. *Acc. Chem. Res.* **2015**, *48*, 1474−1484.
(64) Stevenson, S. M.; Shores, M. P.; Ferreira, E. M. Photooxidizing Chromium Catalysts for Promoting Radical Cation Cycloadditions. *Angew. Chem., Int. Ed.* **2015**, *54*, 6506−6510.
(65) Stevenson, S. M.; Higgins, R. F.; Shores, M. P.; Ferreira, E. M. Chromium Photocatalysis: Accessing Structural Complements to Diels−Alder Adducts with Electron-Deficient Dienophiles. *Chem. Sci.* **2017**, *8*, 654−660.
(66) Higgins, R. F.; Fatur, S. M.; Shepard, S. G.; Stevenson, S. M.; Boston, D. J.; Ferreira, E. M.; Damrauer, N. H.; Rappé, A. K.; Shores, M. P. Uncovering the Roles of Oxygen in Cr(III) Photoredox Catalysis. *J. Am. Chem. Soc.* **2016**, *138*, 5451−5464.
(67) Cheng, M.; Bakac, A. Photochemical Oxidation of Halide Ions by a nitratochromium(III) Complex. Kinetics, Mechanism, and Intermediates. *J. Am. Chem. Soc.* **2008**, *130*, 5600−5605.

DOI: 10.1021/acs.inorgchem.7b02799
Inorg. Chem. XXXX, XXX, XXX−XXX

(68) Ballardini, R.; Varani, G.; Scandola, F.; Balzani, V. Bimolecular Electron Transfer Processes of Electronically Excited tris(2,2′-bipyridine)chromium(III). *J. Am. Chem. Soc.* **1976**, *98*, 7432−7433.
(69) Bolletta, F.; Maestri, M.; Moggi, L.; Balzani, V. Birnolecular Electron Transfer Reactions of Electronically Excited States of Co -Ordination Compounds. *J. Chem. Soc., Chem. Commun.* **1975**, *0*, 901−902.
(70) Juban, E. A.; McCusker, J. K. Ultrafast Dynamics of ^{2}E State Formation in Cr(acac)3. *J. Am. Chem. Soc.* **2005**, *127*, 6857−6865.
(71) Schrauben, J. N.; Dillman, K. L.; Beck, W. F.; McCusker, J. K. Vibrational Coherence in the Excited State Dynamics of Cr(acac)$_3$: Probing the Reaction Coordinate for Ultrafast Intersystem Crossing. *Chem. Sci.* **2010**, *1*, 405−410.
(72) Rossi, M. B.; Piro, O. E.; Castellano, E. E.; Alborés, P.; Baraldo, L. M. Reactivity and Spectroscopy of the {Ru(DMAP)$_5$} Fragment: An {Ru(NH3)$_5$} Analogue. *Inorg. Chem.* **2008**, *47*, 2416−2427.
(73) Alborés, P.; Slep, L. D.; Weyhermüller, T.; Rentschler, E.; Baraldo, L. M. Exchange Coupling across the Cyanide Bridge: Structural and DFT Interpretation of the Magnetic Properties of a Binuclear chromium(III) Complex. *Dalton Trans.* **2006**, *0*, 948−954.
(74) Noviandri, I.; Brown, K. N.; Fleming, D. S.; Gulyas, P. T.; Lay, P. A.; Masters, A. F.; Phillips, L. The Decamethylferrocenium/decamethylferrocene Redox Couple: A Superior Redox Standard to the Ferrocenium/ferrocene Redox Couple for Studying Solvent Effects on. *J. Phys. Chem. B* **1999**, *103*, 6713−6722.
(75) Yamamoto, Y.; Tamaki, Y.; Yui, T.; Koike, K.; Ishitani, O. New Light-Harvesting Molecular Systems Constructed with a Ru(II) Complex and a Linear-Shaped Re(I) Oligomer. *J. Am. Chem. Soc.* **2010**, *132*, 11743−11752.
(76) De Candia, A. G.; Marcolongo, J. P.; Etchenique, R.; Slep, L. D. Widely Differing Photochemical Behavior in Related Octahedral {Ru-NO}^{6} Compounds: Intramolecular Redox Isomerism of the Excited State Controlling the Photodelivery of NO. *Inorg. Chem.* **2010**, *49*, 6925−6930.
(77) Juris, A.; Balzani, V.; Barigeletti, F.; Campagna, S.; Belser, P.; von Zelewsky, A. Ru(II) Polypyridine Complexes: Photophysics, Photochemistry, Electrochemistry Adn Chemiluminescence. *Coord. Chem. Rev.* **1988**, *84*, 85−277.
(78) Sun, Q.; Mosquera-vazquez, S.; Suffren, Y.; Hankache, J.; Amstutz, N.; Max, L.; Daku, L.; Vauthey, E.; Hauser, A. On the Role of Ligand-Field States for the Photophysical Properties of Ruthenium(II) Polypyridyl Complexes. *Coord. Chem. Rev.* **2015**, *282-283*, 87−99.
(79) Wasgestian, H. F. Evidence against the Doublet Hypothesis. The Photolysis of Hexacyanochromate(III) in Dimethylformamide. *J. Phys. Chem.* **1972**, *76*, 1947−1951.
(80) Wright-Garcia, K.; Basinger, J.; Williams, S.; Hu, C.; Wagenknecht, P. S.; Nathan, L. C. Effects of Steric Constraint on chromium(III) Complexes of Tetraazamacrocycles. Chemistry and Excited-State Behavior of 1,4-C$_2$-Cyclam Complexes. *Inorg. Chem.* **2003**, *42*, 4885−4890.
(81) Feldberg, S. W.; Jeftic, L. Chromium(II)-Catalyzed Aquation of hexacyanochromate(III) to pentacyanomonohydroxychromate(III). *J. Phys. Chem.* **1971**, *75*, 2381−2387.
(82) Feldberg, S. W.; Jeftic, L. Nuances of ECE Mechanism. IV. Theory of Cyclic Voltammetry and Chronoamperometry and Electrochemical Reduction of Hexacyanochromate(III). *J. Phys. Chem.* **1972**, *76*, 2439−2446.
(83) Snellenburg, J. J.; Laptenok, S. P.; Seger, R.; Mullen, K. M.; van Stokkum, I. H. M. Glotaran : A Java -Based Graphical User Interface for the R Package TIMP. *J. Stat. Softw.* **2012**, *49*, 1−22.
(84) Mullen, K. M.; van Stokkum, I. H. M. TIMP: An R Package for Modeling Multi-Way Spectroscopic Measurements. *J. Stat. Softw.* **2007**, *18*, 46.
(85) Van Stokkum, I. H. M.; Larsen, D. S.; Van Grondelle, R. Global and Target Analysis of Time-Resolved Spectra. *Biochim. Biophys. Acta, Bioenerg.* **2004**, *1657*, 82−104.
(86) Pieslinger, G. E.; Albores, P.; Slep, L. D.; Coe, B. J.; Timpson, C. J.; Baraldo, L. M. Communication between Remote Moieties in Linear Ru-Ru-Ru Trimetallic Cyanide-Bridged Complexes. *Inorg. Chem.* **2013**, *52*, 2906−2917.
(87) Rossi, M. B.; Abboud, K.; Alborés, P.; Baraldo, L. M. Structural and Spectroscopic Evidence of Strong Electronic Delocalization through a Cyanido Bridge in a Mixed-Valence Os-Ru Complex. *Eur. J. Inorg. Chem.* **2010**, *2010*, 5613−5616.
(88) Spek, A. L. Structure Validation in Chemical Crystallography. *Acta Crystallogr., Sect. D: Biol. Crystallogr.* **2009**, *65*, 148−155.
(89) Sheldrick, G. M. *SHELXS97 and SHELXL97; Programs for Crystal Structure Resolution*; University of Göttingen: Göttingen, Germany, 1997.
(90) Coe, B. J.; Meyer, T. J.; White, P. S. Synthetic and Structural Studies on Trans-Tetrapyridine Complexes of Ruthenium(II). *Inorg. Chem.* **1995**, *34*, 593−602.
(91) Cadranel, A.; Alborés, P.; Yamazaki, S.; Kleiman, V. D.; Baraldo, L. M. Efficient Energy Transfer via the Cyanide Bridge in Dinuclear Complexes Containing Ru(II) Polypyridine Moieties. *Dalton Trans.* **2012**, *41*, 5343−5350.
(92) Gutmann, V. Solvent Effects on the Reactivities of Organometallic Compounds. *Coord. Chem. Rev.* **1976**, *18*, 225−255.
(93) The excited-state lifetimes observed in emission lifetime experiments are slightly shorter than those obtained in transient absorption measurements. It should be noted that we were able to measure the emission lifetimes only at high sample concentrations due to the low emission quantum yields at 350 nm excitation. Under these conditions, doublet−doublet annihilation processes might take place, which could shorten the excited-state lifetimes.
(94) Zinato, E.; Riccieri, P. Pentacyanochromate(III) Complexes ;: Ground- and Excited-State Chemistry. *Coord. Chem. Rev.* **2001**, *211*, 5−24.
(95) Endicott, J. F.; McNamara, P. G.; Buranda, T.; Macatangay, A. V. Electron Transfer Emission in Simple Transition Metal Donor-Acceptor Systems. *Coord. Chem. Rev.* **2000**, *208*, 61−75.
(96) Chen, Y.-J.; Odongo, O. S.; McNamara, P. G.; Szacilowski, K. T.; Endicott, J. F. Metal-to-Metal Electron-Transfer Emission in Cyanide-Bridged Chromium-Ruthenium Complexes: Effects of Configurational Mixing between Ligand Field and Charge Transfer Excited States. *Inorg. Chem.* **2008**, *47*, 10921−10934.
(97) Chromium ions contribute with a spin of 3/2 each, and the {Ru(py)$_4$} core contributes with a spin of 1 if the donor is a ^{3}MLCT state (total spin 4). In the case where the energy donor is a MM′CT state, the chromium fragment of the accepting MM′CT charge transfer has a spin of 1, the ruthenium center has a spin of 1/2, and the remaining chromium has a spin of 3/2 (total spin 3). The acceptor state is either a Cr-centered ^{2}E or ^{2}T state, to which the chromium contributes with a spin of 1/2, while the other chromium contributes with a spin of 3/2 (total spin 2).
(98) Guo, D.; Knight, T. E.; McCusker, J. K. Angular Momentum Conservation in Dipolar Energy Transfer. *Science* **2011**, *334*, 1684−1687.
(99) Bignozzi, C. A.; Roffia, S.; Chiorboli, C.; Davila, J.; Indelli, M. T.; Scandola, F. Oligomeric Dicyanobis(polypyridine)ruthenium(II) Complexes. Synthesis and Spectroscopic and Photophysical Properties. *Inorg. Chem.* **1989**, *28*, 4350−4358.
(100) Bignozzi, C. A.; Paradisi, C.; Roffia, S.; Scandola, F. Optical Electron-Transfer Transitions in Polynuclear Complexes of the Type X(NH$_3$)$_4$RuNCRu(bpy)$_2$CNRu(NH$_3$)$_4$Y^{m+} (X = NH$_3$, Py; Y = NH$_3$, Py; M = 4−6). *Inorg. Chem.* **1988**, *27*, 408−414.
(101) We were unable to prevent photolysis effects on the picosecond experiments for **3**$^{4-}$, so we exclude it from this part of our analysis. DMAP is a very strong π donor, which results in a high t_{2g} energy and which leads to rapid population of low-energy Ru d−d states and, in turn, to photodecomposition. In addition, a typical time scale of a femtosecond measurement is at least 15 min, enough to observe photodecomposition. These effects become more prominent as the experiment proceeds, i.e. as our delay line scans longer delay times, hence seriously affecting the kinetics measured. This is in contrast to microsecond experiments, where the electronically controlled delay times are randomly scanned. This allows for shorter

DOI: 10.1021/acs.inorgchem.7b02799
Inorg. Chem. XXXX, XXX, XXX−XXX

durations for microsecond experiments, where photodecomposition effects are consequently mitigated.
(102) Cadranel, A.; Aramburu Trošelj, B. M.; Yamazaki, S.; Alborés, P.; Kleiman, V. D.; Baraldo, L. M. Emissive Cyanide-Bridged Bimetallic Compounds as Building Blocks for Polymeric Antennae. *Dalton Trans.* **2013**, *42*, 16723−16732.
(103) Following spin conservation arguments, only one MM′CT band is expected in the ground state. This is depicted in Figure 7a.
(104) Cadranel, A.; Tate, J. E.; Oviedo, P. S.; Yamazaki, S.; Hodak, J. H.; Baraldo, L. M.; Kleiman, V. D. Distant Ultrafast Energy Transfer in a Trimetallic {Ru−Ru−Cr} Complex Facilitated by Hole Delocalization. *Phys. Chem. Chem. Phys.* **2017**, *19*, 2882−2893.

DOI: 10.1021/acs.inorgchem.7b02799
Inorg. Chem. XXXX, XXX, XXX−XXX